Multiple-pathway remediation of mercury contamination by a versatile selenite-reducing bacterium

Wang, Xiaonan; He, Zhanfei; Luo, Hongwei; Zhang, Ming; Zhang, Daoyong; Pan, Xiangliang

Published in:
Science of the Total Environment

DOI:
10.1016/j.scitotenv.2017.09.336

Publication date:
2018

Final version published in Science of the Total Environmnet, Vol 615, 15 Feb 2018, pages 615-623
https://doi.org/10.1016/j.scitotenv.2017.09.336

Multiple-pathway Remediation of Mercury Contamination by a Versatile Selenite-reducing Bacterium

Xiaonan Wang [a,c], Zhanfei He[b], Hongwei Luo[b], Ming Zhang[b], Daoyong Zhang [a,b], Xiangliang Pan [a,b*], Geoffrey Michael Gadd[d]

[a]*Xinjiang Key Laboratory of Environmental Pollution and Bioremediation, Xinjiang Institute of Ecology and Geography, Chinese Academy of Sciences, Urumqi 830011, China*.

[b]*College of Environment, Zhejiang University of Technology, Hangzhou 310014, China*.

[c]*University of Chinese Academy of Sciences, Beijing 100049, China*.

[d]*Geomicrobiology Group, School of Life Sciences, University of Dundee, Dundee, DD15EH, Scotland, UK.*

*Author for correspondence: Professor Xiangliang Pan, College of Environment, Zhejiang University of Technology, Hangzhou 310014, China.

E-mail: { HYPERLINK "mailto:panxl@zjut.edu.cn" }

Tel: +86 571 88320634; Fax: +86 571 88320634.

Running title: Multiple-pathway bioremediation of mercury contamination

ABSTRACT

Mercury contamination is a global concern because of its high toxicity, persistence, bioaccumulative nature, long distance transport and wide distribution in the environment. In this study, the efficiency and multiple-pathway remediation mechanisms of Hg^{2+} by a selenite reducing *Escherichia coli* was assessed. *E. coli* can reduce Hg^{2+} to Hg^{+} and Hg^{0} and selenite to selenide at the same time. This makes a multiple-pathway mechanisms for removal of Hg^{2+} from water in addition to biosorption. It was found that when the original Hg^{2+} concentration was 40 μg L^{-1}, 93.2 ± 2.8% of Hg^{2+} was removed from solution by *E. coli*. Of the total Hg removed, it was found that 3.3 ± 0.1% was adsorbed to the bacterium, 2.0 ± 0.5% was bioaccumulated, and 7.3 ± 0.6% was volatilized into the ambient environment, and most (about 80.6 ± 5.7%) Hg was removed as HgSe and HgCl precipitates and Hg^{0}. On one hand, selenite is reduced to selenide and the latter further reacts with Hg^{2+} to form HgSe precipitates. On the other hand Hg^{2+} is successively reduced to Hg^{+}, which forms solid HgCl, and Hg^{0}. This is the report on bacterially transformation of Hg^{2+} to HgSe, HgCl and Hg^{0} via multiple pathways. It is suggested that *E. coli* or other selenite reducing microorganisms are promising candidates for mercury bioremediation of contaminated wastewaters, as well as simultaneous removal of Hg^{2+} and selenite.

Keywords: Bioremediation; bioreduction; biosorption; bioaccumulation; mercury

1. Introduction

Mercury mainly exists as either elemental (Hg^0) or oxidized mercuric (Hg^{2+}) forms in nature. Hg^{2+} is the primary form occurring in water (Ní Chadhain et al., 2006). The toxicity of Hg^{2+} mainly results from the binding of Hg^{2+} to sulfhydryl groups or disulfide groups in proteins and amino acids, leading to inactivation of enzymes (Zahir et al., 2005). In addition, mercury can be methylated to methyl mercury compounds aerobically and also under anoxic conditions by certain sulfate- and iron-reducing bacteria (Gadd and Griffiths, 1978; Bravo et al., 2014). Methylated derivatives are the most toxic species of mercury owing to their lipid solubility, bioaccumulation and biomagnification through food webs (Ní Chadhain et al., 2006). , not only because of its toxicity and bioaccumulation, but also because of its persistence and wide distribution in the environment (Tavares et al., 2016)

Mercury is one of the most toxic metal elements which is not essential to organisms, and the U.S. Environmental Protection Agency (USEPA) has placed it on the primary list of 129 hazardous chemical substances (Zhang, 2014).

The commonly used model bacterium *Escherichia coli*, including genetically engineered strains, has been widely investigated in environmental microbiology, including in the area of mercury and selenium transformations (Pazirandeh et al., 1998). For instance, a modified strain of *E. coli* possessed enhanced uptake limitations for mercury (Bae et al., 2001). *E. coli* can also mediate selenium transformations such as the reduction of selenite to selenide (Turner et al., 1998). If Cd^{2+} is transported into *E. coli*, subsequent reaction with Se^{2-} can result in synthesis of CdSe (Yan et al., 2014).

Mercury and cadmium are in the same column in the Periodic table, and have some similar chemical properties. It can be hypothesized that the bioreduced Se^{2-} produced by *E. coli* could be employed to capture Hg^{2+} in solution.

However, the reaction of Hg^{2+} with selenide is more rapid and therefore may be a more effective mechanism for Hg^{2+} removal from water. Moreover, it is of great interest to capture Hg^{2+} with Se^{2-} or remove selenium and mercury simultaneously, because it should not be overlook that selenium is an important co-existing element with mercury in mercury mining area (Zhang, 2014; Zhang et al., 2014).

Mercury contamination is a global concern because of its high toxicity and global transport. Microbial bioremediation methods have often been proposed as a potential approach to remove mercury ions from water, because of assumed low cost and high efficiency especially at low concentrations. Some microbiological bioremediation methods have already been successfully used to remove heavy metals including Hg^{2+} (Herrego et al., 2005; Gadd, 2010; Yin et al., 2016). Although Biosorption and bioaccumulation of Hg^{2+} have been extensively studied (Gadd, 1993), these technologies have not been successfully applied to engineering application so far because serious problems with separation of small size microbial cells from water and release of mercury from the bioadsorbent after cell death. Much research has also focused on MerA-mediated bacterial reduction of Hg^{2+} to Hg^{0} and subsequent volatilization of the Hg^{0}. However, a major problem is that unless trapped, mercury usually recycles back to the environment in the form of mercury vapour (Wang et al.,

2012). Thus, better methods for mercury remediation should involve trapping of elemental mercury or precipitation which would prevent volatilization (Xiong et al., 2009; Sinha and Khare, 2012). Recently, a few studies show that bacterially generated Se^0 can been used to immobilize Hg^0 based on their reaction (Belzile et al., 2006; Johnson et al., 2008; Lee et al., 2009; Fellowes et al., 2011; Yang et al., 2011; Jiang et al., 2012; Wang et al., 2016).

In the present study, a versatile bacterium *Escherichia coli* that can remove mercury from water via multiple pathways was reported. This special *E. coli* can effectively remediate Hg^{2+} contamination by biosorption, bioaccumulation, bioreduction-volatilization immobilization of by Se^0, precipitation as HgCl, and formation of HgSe by reaction of Hg^{2+} and Se^{2-} at the same time.

In this study, removal of Hg^{2+} through selenite reduction by *E. coli* was investigated. Changes in Hg^{2+} concentration in solution and Hg^0 in the ambient environment were measured. Mercury biosorbed or bioaccumulated by *E. coli* was also extracted and measured. The mercury-containing precipitate was collected and characterized by scanning electron microscopy and energy-dispersive X-ray spectrometry (SEM-EDS), X-ray diffraction (XRD) and X-ray photoelectron spectroscopy (XPS). This research shows that most of the supplied Hg^{2+} was removed from solution through the formation of HgCl, Hg^0 and HgSe, and only a very small fraction was biosorbed or bioaccumulated. Moreover, only a small fraction of mercury was volatilized into the ambient environment. It can be concluded that *E. coli*, or microorganisms with similar properties, may be excellent candidate species for Hg^{2+} bioremediation and the

simultaneous removal of mercury and selenite from contaminated waters.

2. Materials and methods

2.1 Incubation of bacterium

The facultative anaerobe *Escherichia coli* (GIM1.223), purchased from Guangdong Microbiology Culture Centre, was anaerobically cultivated at 30°C in nutrient broth in serum bottles. Anaerobic conditions were achieved using a Whitley DG250 anaerobic workstation (Don Whitley Scientific, Shipley, England). After a 5% (v/v) inoculation, growth of *E. coli* under anaerobic conditions was recorded.

2.2 Resistance of the bacterium to Hg^{2+} toxicity

Resistance of *E. coli* to Hg^{2+} was examined. Bacterial cells were grown at 30°C in the nutrient broth with various concentrations of Hg^{2+} (applied in the form of $HgCl_2$ of analytical grade) and the absorbance at 600 nm of the culture after 18h exposure to mercury was measured (Cui et al., 2009). The OD_{600} of *E. coli* cultures was comparatively analyzed to assess its resistance to Hg^{2+} toxicity.

2.2 Hg^{2+} removal by E. coli from water

E. coli (5%, v/v) was incubated in 100 mL nutrient broth for 18 h at 30°C to reach the stationary phase (OD_{600}=0.88). 5 mL aliquots of the *E. coli* culture were transferred to 93 mL fresh nutrient broth in serum bottles, cultured in an anaerobic workstation for 18 h, prior to 1 mL Na_2SeO_3 and 1mL $HgCl_2$ being added to the medium. The final concentration of Na_2SeO_3 was 15.8 mg L^{-1} (200 μM) and the final concentration of $HgCl_2$ was 40 and 200 μg L^{-1}. Na_2SeO_3 and $HgCl_2$ stock solutions were sterilized by filtering through a 0.22 μm hydrophilic polyestersulfone membrane filter (Xingya, Shanghai, China). At different time intervals, samples were collected and filtered with

0.22 μm hydrophilic polyestersulfone membranes. SeO_3^{2-} and Hg^{2+} in solution were determined by Liquid Chromatography Hydride Generation Atomic Fluorescence Spectrometry (LC-HGAFS) (Jitian, Beijing, China). Mercury- and selenite-containing nutrient broth without inoculation of *E. coli* was used as a control.

2.3 Hg^0 volatilization

To check whether Hg^{2+} was bioreduced to mercury vapour and volatilized into the ambient environment, an experiment was carried out in a 500 mL jar to measure such Hg^0 using a mercury analyzer (Lumex RA915+, Saint Petersburg, Russia) (Fig. 1). Firstly, *E. coli* (5 mL) was transferred into 93 mL fresh nutrient broth containing 200 μM selenite and 40 μg L^{-1} $HgCl_2$. The jar was then sealed with a rubber stopper and removed from the anaerobic chamber. The Hg^0 vapour in the jar was measured every 2 h by recording the concentration of Hg^0 for 5 min at each sampling time to calculate an average value. A $KMnO_4$ solution (5%, w/v) was used to capture mercury-containing waste gas. For the mercury analyzer, the high concentration mode was selected and an additional cell for analysis was used: the sample flow rate was set 1.0 L min^{-1}. Another experimental treatment was added which contained 1.5 wt% NaN_3 to inhibit *E. coli*. In order to investigate the reductive effects of *E. coli*, 40 μg L^{-1} $HgCl_2$ and 40 μg L^{-1} $HgCl_2$ with 1.5 wt% NaN_3 in nutrient broth were separately incubated. Medium containing 40 μg L^{-1} $HgCl_2$ without *E. coli* was used as an abiotic control.

2.4 Mercury associated with bacterial biomass

N_2 was used to purge the medium for 10 min to remove Hg^0 and the bacterial cell pellet was collected to measure mercury adsorbed to and accumulated in *E. coli*. The culture

was centrifuged (6700 g × 15 min) and then washed once with Milli-Q water. After recentrifugation, the pellet was suspended in 5 mL Milli-Q water and sonicated (Hengao Technology, Tianjin, China) for 10 min to desorb the mercury loosely bound to *E. coli*. The cell suspension was then filtered using 0.22 μm hydrophilic polyestersulfone membrane filters and the mercury in the filtrate was measured by LC-HGAFS. The cell pellet was used to measure mercury accumulated in the *E. coli* cells. The cell pellet was suspended in 5 mL HCl (5 mol L^{-1}) for 10 h, and then sonicated for 2 h with shaking several times throughout this period. The suspension was collected by centrifugation (8500 g × 15 min, 4°C). 2 mL filtrate was transferred to a 10 mL tube, and 6 mol L^{-1} NaOH was added drop by drop to modify the pH to 5-7. After this, 0.1 mL L-cysteine solution (10 g L^{-1}) was added to the filtrate which was then diluted with Milli-Q water to 5 mL and then filtered using a 0.22 μm hydrophobic membrane filter. Mercury species and concentration were determined by LC-HGAFS. Three controls were also performed. *E. coli* with 15.8 mg L^{-1} selenite, 40 μg L^{-1} $HgCl_2$, 1.5 wt% NaN_3; *E.coli* with 40 μg L^{-1} $HgCl_2$, and *E. coli* with 40 μg L^{-1} $HgCl_2$, 1.5 wt% NaN_3 were separately incubated in nutrient broth, and the bacterial pellet was collected to measure mercury concentration as described above. A reagent blank without addition of the organism was treated in an identical manner.

2.5 Characterization of the cell pellet and precipitate

The precipitate was characterized using SEM-EDS, XRD and XPS. For SEM-EDS, the precipitate was collected by centrifugation (9700 g x 15 min), washed with Milli-Q water three times, frozen at -80°C for 4 h, and then freeze-dried in a vacuum freeze

dryer (Labconco, Kansas, USA). Samples were coated with gold using a Emitech K575 sputter coater (Emitech Ltd., Ashford Kent, UK), and examined with a scanning electron microscope (Zeiss Super 55VP, Oberkochen, Germany) at accelerating voltages from 15 to 35 kV. Elemental analysis was carried out using energy-dispersive X-ray spectrometry (Bruker XFlash 5010, Berlin, Germany).

For XRD, samples were centrifuged (9700 g × 15 min) and then washed twice with Milli-Q water and acetone, respectively. After recentrifugation, samples were frozen at -80 ^{o}C for 4 h, and then freeze-dried. XRD spectra were obtained using a Bruker D8 diffractometer (Bruker, Karlsruhe, Germany) with a Cu anode (40 kV, 30 mA) scanning from 5 to 80^{0}.

XPS analysis was used to identify the binding energies of different forms of mercury and selenium on the surface of the precipitate, and XPS samples were prepared as described for SEM. XPS were recorded on powders with a Thermos ESCALAB 250Xi spectrometer (Thermo Fisher Scientific, Massachusetts, USA) using an Al Ka monochromatized source. Surface charging effects were corrected with a C 1s peak at 284.8 eV as a reference. Curve fitting and decomposition were achieved assuming Gaussian-Lorentzian fitting following Shirley background subtraction.

2.6 Reagents

All chemicals and reagents used in this study were of analytical grade. Nutrient broth was from Aobo Xing Bio-tech Co., Ltd. (Beijing, China). $HgCl_2$ was from Sino Pharm Chemical Reagents (Shanghai, China), $HgCl_2$ solution was prepared as a 1 g L^{-1} stock solution in Milli-Q water (18 MΩ cm^{-1}), HCl (7%, v/v), HNO_3 (2.4%, v/v) and $K_2Cr_2O_7$

(0.5 g L^{-1}) was added into the stock solution to maintain the oxidation state of mercury. Na_2SeO_3 was supplied by Guang Fu (Tianjin, China) and prepared as a 500 mM stock solution in Milli-Q water.

2.7 Statistical analysis

All experiments were carried out in triplicate; error bars on figures show the standard deviations.

3. Results and discussion

3.1 Resistance of E. coli to Hg^{2+}

The { HYPERLINK "http://dict.cn/facultative%20anaerobe" } *E. coli* grew well under anaerobic conditions (Fig. 2a). *E. coli* shows good resistance to Hg^{2+} (Fig. 2b). Almost no inhibition was observed when Hg^{2+} concentration was below 40 μg L^{-1}. However, when the concentration ranged from 40 to 80 μg L^{-1}, the inhibition increased with increasing concentrations of Hg^{2+}. Growth of *E. coli* was completely inhibited when the concentration of Hg^{2+} was above 80 μg L^{-1}. Since Hg^{2+} concentration in most aquatic environment is at ng L^{-1} or several μg L^{-1}, this *E. coli* can be used for remediation of Hg^{2+} contaminated water.

3.2 Hg^{2+} *removal efficiency*

Concentrations of Hg^{2+} and selenite in the medium decreased sharply as the *E. coli* grew (Fig. 3, 4). About 99.2 ± 0.34% and 93.2 ± 2.8% of Hg^{2+} was removed from solution upon addition of 200 μg L^{-1} and 40 μg L^{-1} Hg^{2+}, respectively. Selenite with an initial concentration of 15.8 ± 0.9 mg L^{-1} was completely removed from solution in the presence of 40 and 200 μg L^{-1} Hg^{2+}. There was little changes of Hg^{2+} and selenite

concentrations for the control.

3.3 Hg^0 volatilization

The amount of mercury which was volatilized into the ambient environment was estimated by integration of the Hg^0 concentration-time curves (Fig. 5). It was found that mercury was readily volatilized into air. For the control, 93.4 ± 8.1 ng (2.3 ± 0.2%) mercury was volatilized into the ambient environment compared with 291.9 ± 23.9 ng (7.3 ± 0.6%) for the experimental treatment. It was found that *E. coli* could reduce Hg^{2+} to Hg^0 vapour while the addition of selenite inhibited volatilization of Hg^0. When supplied with NaN_3, Hg^{2+} reduction decreased because of the inhibition of metabolic activity by *E. coli*. Over 24 h, the Hg^0 concentration decreased to below 5 ng m^{-3} which was similar to concentrations in the ambient environment (3.88 ng m^{-3}).

3.4 Fractions of mercury in the biomass

The species and concentration of mercury in the bacterial cell pellet were classified into two fractions, biosorption and bioaccumulation. Methyl mercury (MeHg) and ethylmercury (EtHg) were not detected. Only Hg^{2+} was found and the concentration values of Hg^{2+} for biosorption and bioaccumulation are shown in Table 1. When supplied with 15.8 mg L^{-1} selenite and 40 μg L^{-1} Hg^{2+}, 132.6 ± 4.2 ng (3.3 ± 0.1%) of Hg^{2+} was adsorbed to cell surface and 81.5 ± 19.4 ng (2.0 ± 0.5%) of Hg^{2+} was accumulated intracellularly. The supply of selenite slightly increased the fractions of biosorption and bioaccumulation. Inactivation of the cells by NaN_3 increased the mercury biosorbed or bioaccumulated.

3.5 Chemical state of Hg and Se

Comparison of the SEM micrographs of *E. coli* in the absence (Fig. 6a) or presence of Hg^{2+} (Fig. 6b), showed that in the presence of mercury and selenite, particles appeared inside the cells. EDS revealed the existence of Se^0 particles (Fig. 6c) which is consistent with the red/orange colour produced. Moreover, some other particles were also formed which were mainly composed of mercury and selenium according to EDS (Fig. 6d, e). Ten particles were selected as shown in Fig. 6d, and the relationship between the atomic concentration (at %) of selenium and mercury were calculated. The atom ratio of selenium and mercury found in these particles was 1.23 (Fig. 6f). Apart from these, some bright droplets were also detected inside the cell in SEM micrographs (Fig. 6g), which are suggested to be elemental mercury based on the EDS analysis (Fig. 6h).

Distinct peaks were found in XRD spectra indicating that the majority of mercury was present as HgCl (PDF#01-0768) (Fig. 7). HgSe (PDF#65-2892) was also observed in the XRD spectrum.

Fig. 8a shows the XPS survey spectrum, showing obvious peaks mainly attributed to C, O, Hg and Se. Fig. 8b shows the high-resolution XPS spectrum of C 1s. This shows an asymmetric peak with a tail between 282 and 291 eV which is a good indication of the presence of C=O, C-O and C-C groups. The high-resolution XPS spectrum of mercury (Fig. 8c) can be curve-fitted into three pairs of Hg4f peaks at 99.5, 100.8 and 101.8 eV, all of which have a spin-orbit splitting of the 4f 7/2 and 4f 5/2 states of 3.9 eV. Mercury could therefore be present as Hg^0, Hg_2Cl_2, HgO and HgS according to published standards (Brinen and McClure, 1972; Nefedov et al., 1980). The Se 3d XPS curve in Fig. 8d shows broad signals ranging from ~52 to 57 eV which indicates the coexistence

of different selenium chemical environments in the cell pellet/precipitate. The peak-fitting for Se 3d is also shown in Fig. 8d. The Se $3d_{5/2}$ and Se $3d_{3/2}$ binding energy was observed at 53.5 eV and 54.3 eV, respectively, which is in good agreement with the binding energy values previously reported for Se^{2-} (Miyake et al., 1984; Nelson et al., 1991). The $Se3d_{5/2}$ and Se $3d_{3/2}$ binding energy was observed at 54.6 eV and 55.4 eV, respectively, which is in good agreement with the binding energy values previously reported for Se^{0} (Mårtensson et al., 1982). The results of XPS revealed that mercury occurred as Hg^{0}, Hg^{1+} and Hg^{2+}, while selenium was present as Se^{0} and Se^{2-}.

Previous work has reported that *E.coli* can exhibit a high resistance to selenium and cadmium (Yan et al., 2014). Even though mercury is toxic and not essential to organisms, some bacteria can also exhibit resistance to mercury. In this work, it was found that growth of *E.coli* was not inhibited below 40 μg L^{-1} Hg^{2+}, so it is feasible that this bacterium could be used in the treatment of low concentrations of mercury. In order to remove Hg^{2+} from solution, *E.coli* was cultured with $HgCl_2$ and Na_2SeO_3 in liquid medium. After about 1 h, the medium changed to a red/orange colour due to the formation of elemental selenium which was confirmed by EDS measurements. Moreover, the addition of mercury did not inhibit selenite reduction and almost all of the selenite was removed from solution. It is known that, *E. coli* can reduce selenite to selenide, the mechanism of which being considered to be related to glutathione metabolism (Leinfelder et al., 1988; Turner et al., 1998). After 18 h, *E.coli* reached the stationary phase of growth when glutathione would be synthesized. The formation of glutathione can be regarded as a detoxification mechanism because it can reduce

inorganic materials to biologically less toxic forms (Apontoweil and Berends, 1975; Greer and Perham, 1986). With the synthesis of glutathione, selenite taken up by *E.coli* was reduced to selenide, some of which was further transformed to Se^0. However, some of the selenide could be captured by Hg^{2+}, and the EDS results demonstrated the formation of HgSe. Selenide rarely exists in natural environments. It has been reported that Cd^{2+} inside *E.coli* could capture selenide resulting in the formation of CdSe, which has been used to synthesize CdSe quantum dots (Yan et al., 2014). Mercury and cadmium are in the same column in the Periodic table, and the properties of these two elements are similar to a certain extent. It is likely that bioreduced Se^{2-} could also be employed to capture Hg^{2+} from water, and this study supports this assumption. In previous work, selenium has been used to capture mercury because of the formation of HgSe, with the atom ratio between selenium and mercury being close to 1 (Yang et al., 2011). In the present study, precipitated particles mainly contained selenium and mercury with an atom ratio, calculated according to EDS spectra, of approximately 1.23, which also suggested the presence of HgSe. The atom ratio between selenium and mercury is a little higher than 1 possibly because of the effect of Se^0 which was formed when selenite was added. The XRD patterns also demonstrated the formation of HgSe. Thus, these experiments have shown that bioreduced Se^{2-} can react with Hg^{2+} leading to the formation of HgSe. The present study is consistent with previous studies, Truong et al. (2014) found the formation of inert HgSe by *Desulfovibrio desulfuricans* in the presence of selenite and Hg prevented the entrance of Hg into the cell as well as reduced the bioavilability of Hg for biomethylation.

SEM-EDS and XRD also revealed the formation of HgCl and elemental mercury droplets, with XPS demonstrating the presence of Se^0, Se^{2-}, Hg^{1+}, Hg^{2+} and Hg^0. This is because a fraction of the Hg^{2+} was reduced to Hg^0. Hg^{2+} is a main species of mercury in aquatic solution, and $HgCl_2$ is a common compound of mercury. However, HgCl does not regularly exist in the environment and is rarely reported in papers. Nazhat and Asmus (1973) found that $HgCl_2$ could be reduced by hydrated electrons and reducing radicals to form HgCl. Hg_2Cl_2 is a more common compound in the environment which is formed by dimerization of HgCl (Nazhat and Asmus, 1973). Both Hg_2Cl_2 and HgCl form precipitates in aquatic solution which can therefore stably exist in the environment. In this study, a consequence of the reaction between selenite and glutathione was the production of superoxide (Turner et al., 1998; Bébien et al., 2002). Superoxide is a very redox-active species owing to the presence of an unpaired electron and has been reported to be involved in the reduction process. Superoxide is able to reduce silver ions with resultant production of Ag nanoparticles (Jones et al., 2011). Superoxide can also mediate Fe(Ⅲ) reduction resulting in the production of iron(Ⅱ) (Rose and Waite, 2005). Thus we can hypothesize that superoxide may be connected to the reduction of Hg^{2+}. This may also be related to light, because light-induced transformations of mercury species also occurs in the environment (Nriagu, 1994). The mechanism of these processes are not yet clear, and more research is needed to further understand the mechanisms involved.

In this study, Hg^{2+} was not only reduced to Hg^+, which is precipitated as HgCl, but also reduced to elemental mercury (Hg^0) droplets. Previous work has already reported the

formation of mercury droplets. *Pseudomonas putida* was used to remove mercury from contaminated water and soil, and it was found that some mercury accumulated in the gel matrix of immobilized beads as mercury droplets (Okino et al., 2001). Sinha (2011) found that mercury transformation by an *Enterobacter* sp. resulted in simultaneous synthesis of mercury nanoparticles which prevented mercury recycling back to the atmosphere (Sinha and Khare, 2011). This is in agreement with this study where small mercury droplets were synthesized, but only 7.3% of mercury was volatilized into the ambient environment.

Biosorption and bioaccumulation are two important methods for mercury removal from solution. A large number of bacteria have been reported to be capable of mercury biosorption, and bioaccumulation of mercury is a well-known phenomenon in aquatic environments and considered to be the main mechanism for human mercury exposure. A lack of specificity and lower robustness of biomass based systems are often cited as major disadvantages for biosorption, and biosorbed mercury could readily to go back into the environment (Gadd, 2009; Fomina and Gadd, 2014). A major drawback of bioaccumulation is inhibition of cell growth which will influence mercury removal. Biosorption and bioaccumulation of Hg^{2+} were detected in this work and accounted for 3.3 ± 0.1% and 2.0 ± 0.5% of removal, respectively, which is small and did not significantly inhibit the overall removal of Hg^{2+} from solution.

The method described in this study can be applied to simultaneous removal of mercury and selenite. Selenium is another common potentially toxic pollutant (Dungan et al., 2003). Selenium contamination is frequently present in mixed metal polluted waste

(Hockin and Gadd, 2006), and selenium pollution in mercury mining areas must be considered (Zhang, 2014). Mining activities have led to a large amount of mercury and selenium being released into the surrounding environment (Horvat et al., 2003). Selenium released into local paddy soil mainly arose from the leaching of selenium from mercury-mining waste (Zhang et al., 2014). Although biotechnologies that can remove mercury or selenium separately have been developed, no technologies have been developed that simultaneously remove mercury and selenium using a single species of microorganism. A cost effective microbiological method as described in this work could be a useful approach to clean up wastewater contaminated by mercury and selenium. However, high efficiency of laboratory experiments does not means similar performance for real waste water treatment in large scale, since more environmental parameters have to be taken into consideration under real conditions. Thus more work are necessary in the future.

4. Conclusions

It was demonstrated that selenite-reducing *E.coli* could remove Hg^{2+} from water via multiple pathways with the formation of HgCl, Hg^0 and HgSe. 93.2 ± 2.8% of the supplied mercury was removed from solution through such transformations. It was found that ~3.3 ± 0.1% was adsorbed to *E. coli*, ~2.0 ± 0.5% was bioaccumulated, ~7.3 ± 0.6% was volatilized into the ambient environment, and the remaining ~80.6 ± 5.7% was precipitated. It is suggested that *E.coli* could be an effective microorganism for Hg^{2+} and selenium removal from contaminated water.

Acknowledgements

This work was supported by the National Natural Science Foundation of China (U1503281 and U1403181). G. M. Gadd also gratefully acknowledges an award (NE/M01090/1) under the National Environmental Research Council (UK) Security of Supply of Mineral Resources Grant Program: Tellurium and Selenium Cycling and Supply (TeASe).

Conflict of Interest Disclosure

The authors declare no competing financial interest.

References

Apontoweil, P., Berends, W., 1975. Glutathione biosynthesis in *Escherichia coli* K 12 properties of the enzymes and regulation. Biochim. Biophys. Acta 399, 1-9.

Bae, W., Mehra, R.K., Mulchandani, A., Chen, W., 2001. Genetic engineering of *Escherichia coli* for enhanced uptake and bioaccumulation of mercury. Appl. Environ. Microbiol. 67, 5335-5338.

Bébien, M., Lagniel, G., Garin, J., Touati, D., Verméglio, A., Labarre, J., 2002. Involvement of superoxide dismutases in the response of *Escherichia coli* to selenium oxides. J. Bacteriol. 184, 1556-1564.

Belzile, N., Wu, G., Chen, Y., Appanna, V.D., 2006. Detoxification of selenite and mercury by reduction and mutual protection in the assimilation of both elements by *Pseudomonas fluorescens*. Sci. Total Environ. 367, 704-714.

Bravo, A.G., Cosio, C., Amouroux, D., Zopfi, J., Chevalley, P.A., Spangenberg, J.E., Ungureanu, V.G., Dominik, J., 2014. Extremely elevated methyl mercury levels in water, sediment and organisms in a Romanian reservoir affected by release of mercury from a chlor-alkali plant. Water Res. 49, 391-405.

Brinen, J., McClure, J., 1972. Trace analysis by ESCA-electrochemical measurements. Anal. Lett. 5, 737-743.

Cui, R., Liu, H., Xie, H., Zhang, Z., Yang, Y., Pang, D., Xie, Z., Chen, B., Hu, B., Shen, P., 2009. Living yeast cells as a controllable biosynthesizer for fluorescent quantum dots. Adv. Funct. Mater. 19, 2359-2364.

Dungan, R.S., Yates, S.R., Frankenberger, W.T., 2003. Transformations of selenate and selenite by *Stenotrophomonas maltophilia* isolated from a seleniferous agricultural drainage pond sediment. Environ. Microbiol. 5, 287-295.

Fellowes, J., Pattrick, R., Green, D., Dent, A., Lloyd, J., Pearce, C., 2011. Use of biogenic and abiotic elemental selenium nanospheres to sequester elemental mercury released from mercury contaminated museum specimens. J. Hazard. Mater. 189, 660-669.

Fomina, M., Gadd, G.M., 2014. Biosorption: current perspectives on concept, definition and application. Bioresour. Technol. 160, 3-14.

Gadd, G.M., 1993. Microbial formation and transformation of organometallic and organometalloid compounds. FEMS Microbiol. Rev. 11, 297-316.

Gadd, G.M., 2009. Biosorption: critical review of scientific rationale, environmental importance and significance for pollution treatment. J. Chem. Technol. Biotechnol. 84, 13-28.

Gadd, G.M., 2010. Metals, minerals and microbes: geomicrobiology and bioremediation. Microbiology 156, 609-643.

Gadd, G.M., Griffiths, A.J., 1978. Microorganisms and heavy metal toxicity. Microb. Ecol. 4, 303-317.

Greer, S., Perham, R.N., 1986. Glutathione reductase from *Escherichia coli*: cloning and sequence analysis of the gene and relationship to other flavoprotein disulfide oxidoreductases. Biochemistry 25, 2736-2742.

Herrero, R., Lodeiro, P., Rey-Castro, C., Vilariño, T., De Vicente, M.E.S., 2005.

Removal of inorganic mercury from aqueous solutions by biomass of the marine macroalga *Cystoseira baccata*. Water Res. 39, 3199-3210.

Hockin, S., Gadd, G.M., 2006. Removal of selenate from sulfate-containing media by sulfate-reducing bacterial biofilms. Environ. Microbiol. 8, 816-826.

Horvat, M., Nolde, N., Fajon, V., Jereb, V., Logar, M., Lojen, S., Jacimovic, R., Falnoga, I., Qu, L., Faganeli, J., Drobne, D., 2003. Total mercury, methylmercury and selenium in mercury polluted areas in the province Guizhou, China. Sci. Total Environ. 304, 231-256.

Jiang, S., Ho, C.T., Lee, J.H., van Duong, H., Han, S., Hur, H.G., 2012. Mercury capture into biogenic amorphous selenium nanospheres produced by mercury resistant *Shewanella putrefaciens* 200. Chemosphere 87, 621-624.

Johnson, N.C., Manchester, S., Sarin, L., Gao, Y., Kulaots, I., Hurt, R.H., 2008. Mercury vapor release from broken compact fluorescent lamps and in situ capture by new nanomaterial sorbents. Environ. Sci. Technol. 42, 5772-5778.

Jones, A.M., Garg, S., He, D., Pham, A.N., Waite, T.D., 2011. Superoxide-mediated formation and charging of silver nanoparticles. Environ. Sci. Technol. 45, 1428-1434.

Lee, B., Sarin, L., Johnson, N.C., Hurt, R.H., 2009. A nano-selenium reactive barrier approach for managing mercury over the life-cycle of compact fluorescent lamps. Environ. Sci. Technol. 43, 5915-5920.

Leinfelder, W., Forchhammer, K., Zinoni, F., Sawers, G., Mandrand-Berthelot, M., Böck, A., 1988. *Escherichia coli* genes whose products are involved in selenium

metabolism. J. Bacteriol. 170, 540-546.

Mårtensson, N., Reihl, B., Vogt, O., 1982. Binding energies and heat-of-formation data for USb_xTe_{1-x} and UAs_xSe_{1-x} compounds as derived from photoelectron spectroscopy. Phys. Rev. B Condens. Matter. Mater Phys. 25, 824.

Miyake, I., Tanpo, T., Tatsuyama, C., 1984. XPS Study on the Oxidation of InSe. Jpn. J. Appl. Phys. 23, 172.

Ní Chadhain, S.M., Schaefer, J.K., Crane, S., Zylstra, G.J., Barkay, T., 2006. Analysis of mercuric reductase (merA) gene diversity in an anaerobic mercury-contaminated sediment enrichment. Environ. Microbiol. 8, 1746-1752.

Nazhat, N., Asmus, K., 1973. Reduction of mercuric chloride by hydrated electrons and reducing radicals in aqueous solutions. Formation and reactions of mercury chloride (HgCl). J. Phys. Chem. 77, 614-620.

Nefedov, V., Salyn, Y.V., Solozhenkin, P., Pulatov, G.Y., 1980. X-ray photoelectron study of surface compounds formed during flotation of minerals. Surf. Interface Anal. 2, 170-172.

Nelson, A.J., Gebhard, S., Kazmerski, L., Colavita, E., Engelhardt, M., Höchst, H., 1991. Formation and Schottky barrier height of Au contacts to $CuInSe_2$. J. Vac. Sci. Technol. A 9, 978-982.

Nriagu, J.O., 1994. Mechanistic steps in the photoreduction of mercury in natural waters. Sci. Total Environ. 154, 1-8.

Okino, S., Iwasaki, K., Yagi, O., Tanaka, H., 2001. Removal of mercuric chloride by immobilized cells of genetically modified *Pseudomonas putida*

PpY101/pSR134. J. Environ. Biotechnol. 1, 41-47.

Pazirandeh, M., Wells, B.M., Ryan, R.L., 1998. Development of bacterium-based heavy metal biosorbents: enhanced uptake of cadmium and mercury by *Escherichia coli* expressing a metal binding motif. Appl. Environ. Microbiol. 64, 4068-4072.

Rose, A.L., Waite, T.D., 2005. Reduction of organically complexed ferric iron by superoxide in a simulated natural water. Environ. Sci. Technol. 39, 2645-2650.

Sinha, A., Khare, S.K., 2011. Mercury bioaccumulation and simultaneous nanoparticle synthesis by *Enterobacter* sp. cells. Bioresour. Technol. 102, 4281-4284.

Sinha, A., Khare, S.K., 2012. Mercury bioremediation by mercury accumulating *Enterobacter* sp. cells and its alginate immobilized application. Biodegradation 23, 25-34.

Truong, H.Y.T., Chen, Y., Saleh, M., Nehzati, S., George, G.N., Pickering, I.J., Belzile, N., 2014. Proteomics of *Desulfovibrio desulfuricans* and X-ray absorption spectroscopy to investigate mercury methylation in the presence of selenium. Metallomics 6, 465-475.

Tavares, D.S., Lopes, C.B., Daniel-da-Silva, A.L., Vale, C., Trindade, T., Pereira, M.E., 2016. Mercury in river, estuarine and seawaters–is it possible to decrease realist environmental concentrations in order to achieve environmental quality standards? Water Res. 106, 439-449.

Turner, R.J., Weiner, J.H., Taylor, D.E., 1998. Selenium metabolism in *Escherichia coli*. Biometals 11, 223-227.

Wang, J., Feng, X., Anderson, C.W., Xing, Y., Shang, L., 2012. Remediation of mercury

contaminated sites–a review. J. Hazard. Mater. 221, 1-18.

Wang, X., Zhang, D., Pan, X., Lee, D.J., Al-Misned, F.A., Mortuza, M.G., Gadd, G.M., 2017. Aerobic and anaerobic biosynthesis of nano-selenium for remediation of mercury contaminated soil. Chemosphere 170, 266-273.

Xiong, Z., He, F., Zhao, D., Barnett, M.O., 2009. Immobilization of mercury in sediment using stabilized iron sulfide nanoparticles. Water Res. 43, 5171-5179.

Yan, Z., Qian, J., Gu, Y., Su, Y., Ai, X., Wu, S., 2014. Green biosynthesis of biocompatible CdSe quantum dots in living *Escherichia coli* cells. Mater. Res. Express 1, 015401.

Yang, D., Chen, Y., Belzile, N., 2011. Evidences of non-reactive mercury–selenium compounds generated from cultures of *Pseudomonas fluorescens*. Sci. Total Environ. 409, 1697-1703.

Yin, K., Lv, M., Wang, Q., Wu, Y., Liao, C., Zhang, W., Chen, L., 2016. Simultaneous bioremediation and biodetection of mercury ion through surface display of carboxylesterase E2 from *Pseudomonas aeruginosa* PA1. Water Res. 103, 383-390.

Zahir, F., Rizwi, S.J., Haq, S.K., Khan, R.H., 2006. Low dose mercury toxicity and human health. Environ. Toxicol. Pharmacol. 20, 351-360.

Zhang, H., 2014. Impacts of Selenium on the Biogeochemical Cycles of Mercury in Terrestrial Ecosystems in Mercury Mining Areas. Springer.

Zhang, H., Feng, X., Jiang, C., Li, Q., Liu, Y., Gu, C., Shang, L., Li, P., Lin, Y., Larssen, T., 2014. Understanding the paradox of selenium contamination in mercury

mining areas: high soil content and low accumulation in rice. Environ. Pollut. 188, 27-36.

Table 1. Amount of mercury associated with biosorption and bioaccumulation processes in mercury removal by *E. coli*. 1.5 wt% NaN_3 was added to inhibit the metabolic activity of *E. coli*. Experiments were carried out in triplicate, and the values shown are means of three measurements ± standard deviation.

	Biosorption		Bioaccumulation		Total	
	Hg^{2+} (ng)	wt%	Hg^{2+} (ng)	wt%	Hg^{2+} (ng)	wt%
E. coli + Hg^{2+}	44.5±5.4	1.11±0.14	43.5±7.5	1.09±0.19	88.0±12.9	2.20±0.32
E. coli + Hg^{2+} + NaN_3	111.5±18.8	2.79±0.47	32.8±15.1	0.82±0.38	144.3±33.9	3.61±0.85
E. coli + Se^{4+} + Hg^{2+}	132.6±4.2	3.32±0.11	81.5±19.4	2.04±0.49	214.1±23.6	5.35±0.59
E. coli + Se^{4+} + Hg^{2+} + NaN_3	535.3±24.5	13.38±0.61	200.8±39.7	5.02±0.99	736.1±64.2	18.4±1.61

Figure Legends

Fig. 1. The experimental setup for analyzing Hg^0 volatilization into the ambient environment.

Fig. 2. Growth of *E. coli* under anaerobic conditions without Hg^{2+} (a) and the dependence of biomass production on the concentration of Hg^{2+} under anaerobic conditions (b). Error bars (n=3) represent the standard deviation.

Fig. 3. Changes in Hg^{2+} concentration in medium with or without *E. coli* (control) as a function of incubation time in the presence of 40 or 200 μg L^{-1} Hg^{2+}. Symbols represent: (□) Hg^{2+} in control, initial Hg^{2+} concentration 200 μg L^{-1}; (■) Hg^{2+} in the presence of *E. coli*, initial concentration Hg^{2+} 200 μg L^{-1}; (▽) Hg^{2+} in control, initial Hg^{2+} concentration 40 μg L^{-1}; (▼) Hg^{2+} in the presence of *E. coli*, initial Hg^{2+} concentration 40 μg L^{-1}. Error bars (n=3) represent the standard deviation.

Fig. 4. Change in selenite concentration in medium with or without *E. coli* (control) as a function of incubation time in the presence of 15.8 mg L^{-1} selenite and 40 or 200 μg L^{-1} $HgCl_2$. Symbols represent: (□) selenite in control, initial Hg^{2+} concentration 200 μg L^{-1}; (■) selenite in the presence of *E. coli*, initial Hg^{2+} concentration 200 μg L^{-1}; (▽) selenite in control, initial Hg^{2+} concentration 40 μg L^{-1}; (▼) selenite in the presence of *E. coli*, initial Hg^{2+} concentration 40 μg L^{-1}. Error bars (n=3) represent the

standard deviation.

Fig. 5. Hg^0 volatilized into the ambient environment as determined using a Lumex RA915+ mercury analyzer. Symbols represent: (■) Hg^0 volatilized into the ambient environment in the presence of 40 μg L^{-1} $HgCl_2$ and 15.8 mg L^{-1} selenite. (●) Hg^0 volatilized into the ambient environment in the presence of 40 μg L^{-1} $HgCl_2$, 15.8 mg L^{-1} selenite and 1.5 wt% NaN_3. (▲) Hg^0 volatilized into the ambient environment in the presence of 40 μg L^{-1} $HgCl_2$. (▼) Hg^0 volatilized into the ambient environment in the presence of 40 μg L^{-1} $HgCl_2$ and 1.5 wt% NaN_3. (◆) Hg^0 volatilized into the ambient environment in the uninoculated control, which contained 40 μg L^{-1} $HgCl_2$. Error bars (n=3) represent the standard deviation.

Fig. 6. SEM micrograph of *E. coli* and SEM-EDS micrographs of *E. coli* in the presence of selenite and Hg^{2+}. (a) SEM micrograph (scale bar = 1 μm) of *E. coli*. (b) SEM micrograph (scale bar = 200 nm) of *E. coli* after growth in the presence of 15.8 mg L^{-1} selenite, 40 and 200 μg L^{-1} $HgCl_2$. (c) EDS spectrum of the particles shown in (b). (d) SEM micrograph (scale bar = 200 nm) of *E. coli* after growth in the presence of 15.8 mg L^{-1} selenite, 40 and 200 μg L^{-1} $HgCl_2$. (e) EDS spectrum of the particles shown in (d). (f) The relationship between the atom concentration (at %) of selenium and mercury in ten particles shown in (d). (g) SEM micrograph (scale bar = 2 μm) of *E. coli* grown in the presence of 15.8 mg L^{-1} selenite, 40 and 200 μg L^{-1} $HgCl_2$. (h) EDS spectrum of the droplets shown in (g). Typical micrographs are shown from one of several

determinations.

Fig. 7. XRD pattern of the precipitate from *E. coli* inoculated medium with the addition of 200 mM selenite, 40 and 200 μg L^{-1} $HgCl_2$. (a) XRD pattern of the sample; (b) Standard XRD pattern of HgCl (PDF#01-0768); (c) Standard XRD pattern of HgSe (PDF#65-2892). Typical patterns are shown from one of two determinations both of which gave similar results.

Fig. 8 XPS spectra of the precipitation. (a) XPS survey spectra; (b) high-resolution XPS spectra of C 1s; (c) high-resolution XPS spectra of Hg 4f; (d) high-resolution XPS spectra of Se 3d. Symbols represent: dot line refers to experimental spectrum; solid line refers to interpolate spectrum; dash line refers to fitted peaks; dash dot line refers to background. Typical results are shown from one of several determinations.

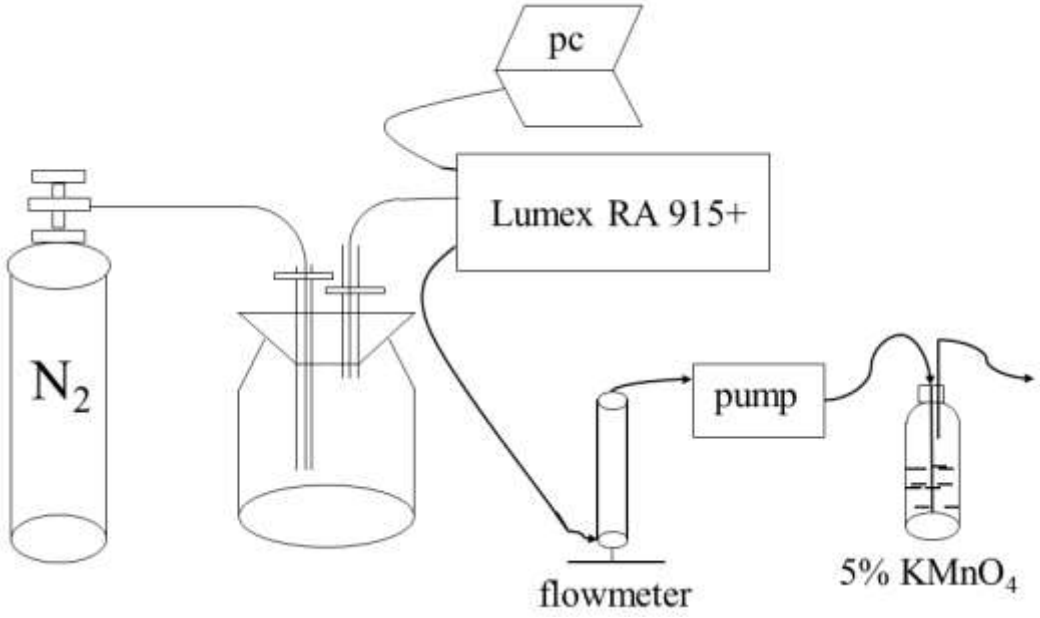

Fig. 1

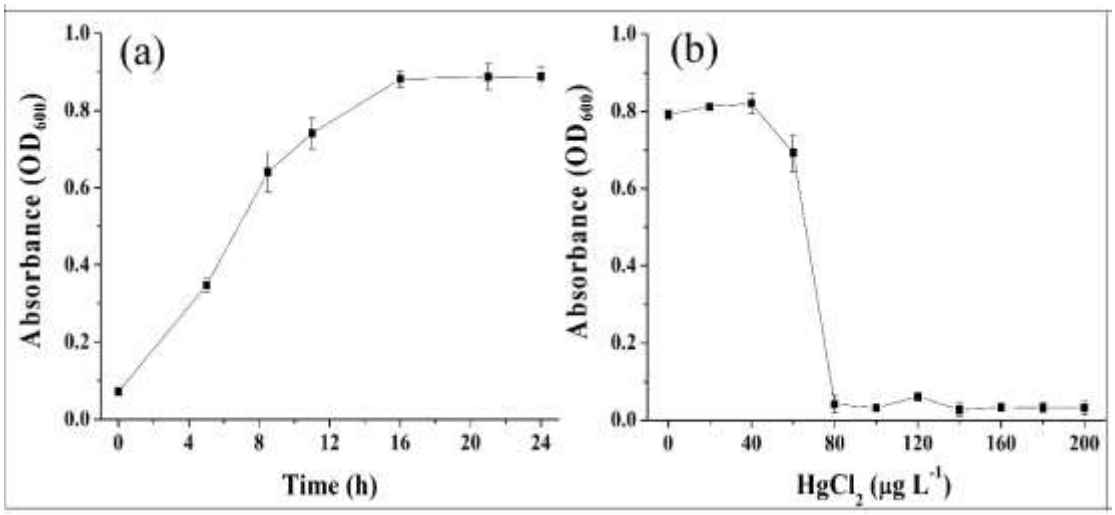
(a)
Absorbance (OD600)
1.0
0.8
0.6
0.4
0.2
0.0
0
4
8
12
16
20
24
Time (h)
(b)
Absorbance (OD600)
1.0
0.8
0.6
0.4
0.2
0.0
0
40
80
120
160
200
HgCl2 (μg L-1)

Fig. 2

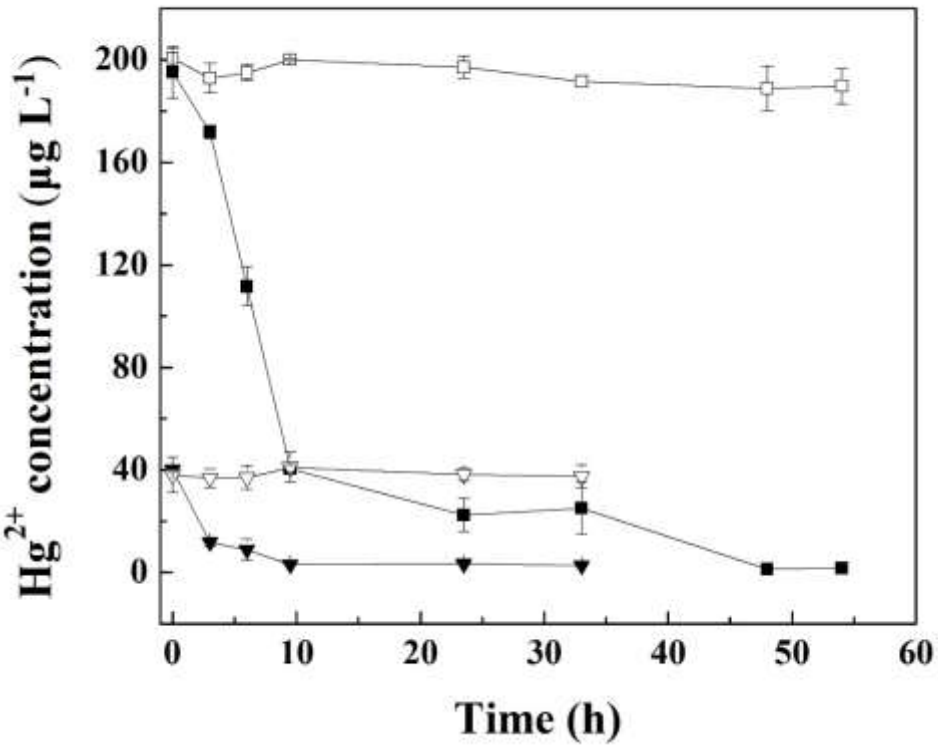
Hg2+ concentration (μg L-1)
200
160
120
80
40
0
0
10
20
30
40
50
60
Time (h)

Fig. 3

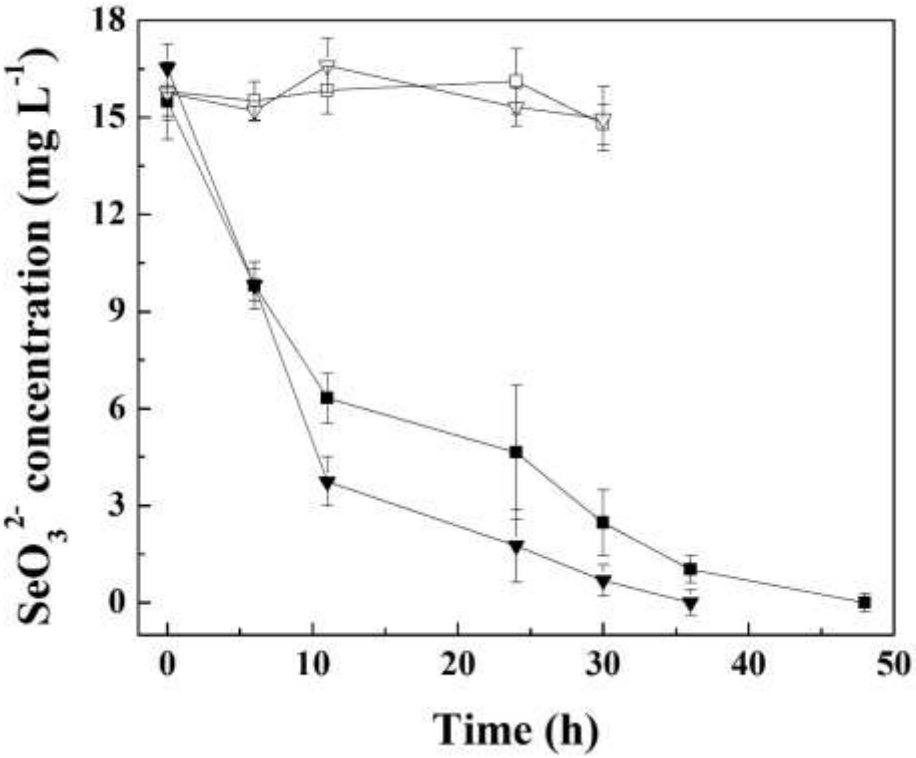

Fig. 4

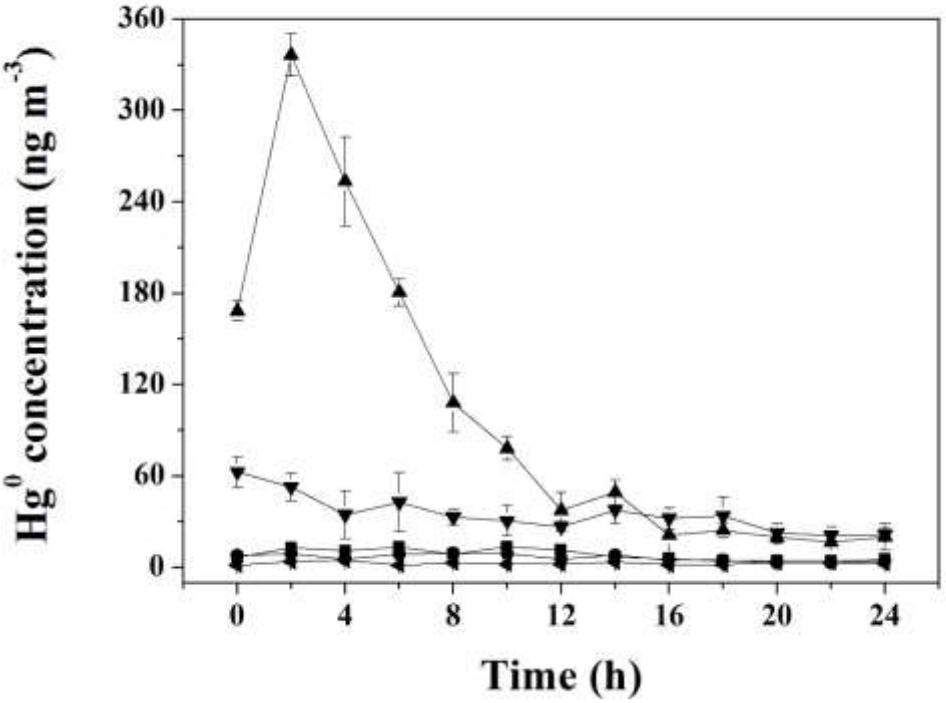
360
300
240
180
120
60
0
Hg0 concentration (ng m-3)
0
4
8
12
16
20
24
Time (h)

Fig. 5

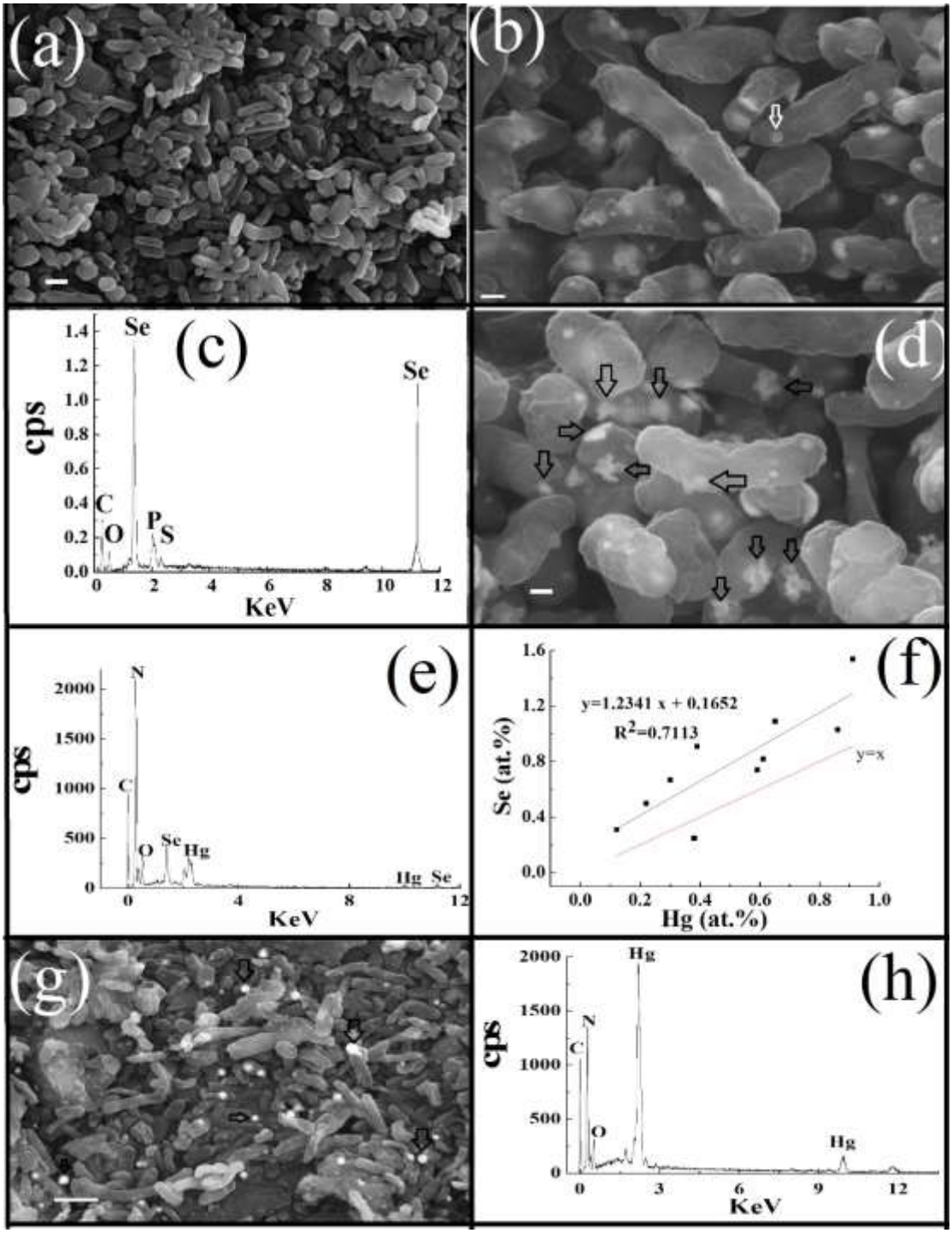
(a)
(b)
(c)
Se
Se
C
O
P
S
cps
KeV
(d)
(e)
N
C
O
Se
Hg
Hg Se
cps
KeV
(f)
y=1.2341 x + 0.1652
R2=0.7113
y=x
Se (at.%)
Hg (at.%)
(g)
(h)
Hg
N
C
O
Hg
cps
KeV

Fig. 6

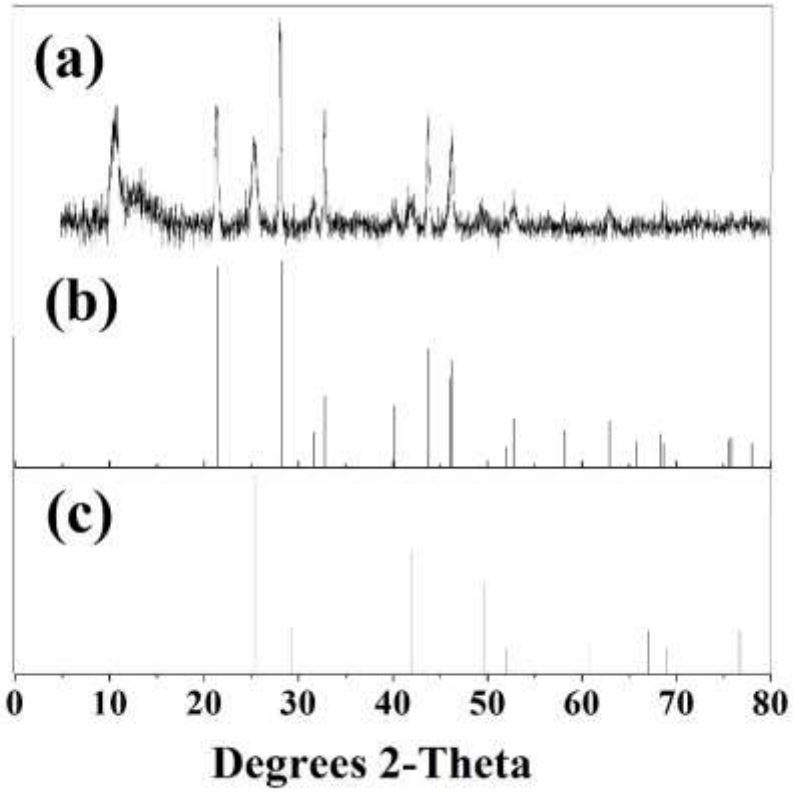

Fig. 7

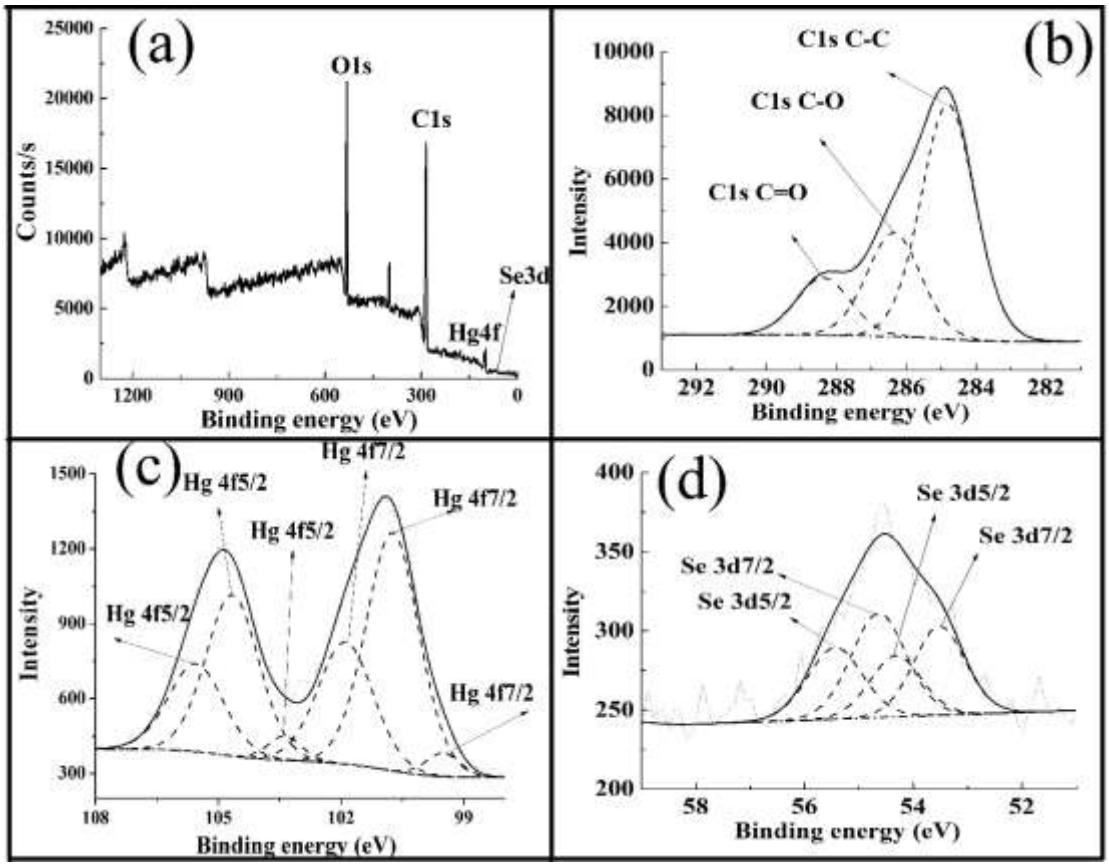
(a)
O1s
C1s
Se3d
Hg4f
Counts/s
Binding energy (eV)
(b)
C1s C-C
C1s C-O
C1s C=O
Intensity
Binding energy (eV)
(c)
Hg 4f5/2
Hg 4f7/2
Hg 4f5/2
Hg 4f7/2
Hg 4f5/2
Hg 4f7/2
Intensity
Binding energy (eV)
(d)
Se 3d5/2
Se 3d7/2
Se 3d7/2
Se 3d5/2
Intensity
Binding energy (eV)

Fig. 8